

## A LATTICE-PARTICLE APPROACH FOR THE SIMULATION OF FRACTURE PROCESSES IN FIBER-REINFORCED HIGH-PERFORMANCE CONCRETE

FRANCISCO MONTERO-CHACÓN<sup>\*,†</sup>, ERIK SCHLANGEN<sup>‡</sup> AND FERNANDO MEDINA<sup>†</sup>

<sup>\*</sup> Abengoa Research  
Campus Palmas Altas, Energía Solar 1, 41014 Seville, Spain  
e-mail: francisco.montero@research.abengoa.com, www.abengoa.com

<sup>†</sup> E.T.S. de Ingeniería, Universidad de Sevilla  
Camino de los Descubrimientos s/n, 41092 Seville, Spain  
e-mail: {fmchacon,medinaencina}@us.es, www.esi.us.es

<sup>‡</sup> Microlab, CITG, Delft University of Technology  
Stevinweg 1, 2628 CN Delft, The Netherlands  
e-mail: h.e.j.g.schlangen@tudelft.nl, www.tudelft.nl

**Key words:** Lattice-particle model, Fiber Reinforced Concrete, FRHPC, Pull-out test, Fracture

**Abstract:** The use of fiber-reinforced high-performance concrete (FRHPC) is becoming more extended; therefore it is necessary to develop tools to simulate and better understand its behavior. In this work, a discrete model for the analysis of fracture mechanics in FRHPC is presented. The plain concrete matrix, made of mortar and coarse aggregates, is modeled by means of a three-dimensional random particle model. The fiber inclusions are modeled as truss elements linked to the matrix via special interface elements. Fiber pull-out tests are performed to characterize the interface behavior and implemented into direct tension tests with different fiber configurations.

### 1 INTRODUCTION

New requirements for construction materials have led to the development of the so-called fiber-reinforced high-performance concrete (FRHPC), by which different benefits over traditionally concrete can be obtained (e.g. improvement on mechanical properties, maintenance reduction, and extend life cycle among others).

The use of fiber-reinforced high-performance concrete (FRHPC) is nowadays widely extended. The inclusion of fibers inside the quasi-brittle concrete matrix enhances the mechanical properties (e.g. strength, toughness, fatigue life) of the new resulting composite material. Different types of fibers (e.g. steel, PVA, PP, wood) have been used, and are currently subject of study [1].

Therefore, there is a clear need in developing new numerical tools to aid the materials engineer in the design of these new materials.

In general, the mechanical response of the FRHPC material depends on fibre parameters (size, stiffness, strength, volume content and shape), matrix parameters (stiffness, strength and fracture energy), and fiber-matrix bond parameters (bond strength, stiffness and debonding energy). These parameters can be measured experimentally by means of pull-out tests [2].

In this work, a discrete model, namely a lattice-particle approach, is presented for the analysis of fracture mechanics in FRHPC. Based on the aforementioned parameters, a three-dimensional numerical model is provided for the design of FRHPC. Due to the

lack of experimental data of the fiber-matrix interface, the bond properties are obtained through pull-out tests and different global material behaviour, ranging from softening to hardening, can be obtained.

## 2 FIBER-REINFORCED LATTICE-PARTICLE MODEL

Discrete models have been proven as an efficient approach to model fracture processes in quasi-brittle materials [3-7].

One main issue concerning the discrete models is that, depending on its nature, an important number of degrees of freedom (dofs) may be required. This is especially important when dealing with additional phases. For this reason, it is important to use an appropriate discrete model. In this sense, a lattice-particle approach [4,5,7] seems to be a valid choice, since the matrix nodes are defined as the centroids of the aggregates, lightening the total number dofs.

Different approaches to model fiber-reinforced cementitious composites can be found in the literature, many of them as a new feature of previously validated discrete models [8-12]. Schlangen et al. [8] included fibers to the original lattice model. The fibers were linked to the matrix lattice via interface elements. These elements were supposed to fail under brittle tension or compression [8] but ductile response was later implemented [12]. Another type of fiber-reinforced lattice model is that of Bolander and Saito [9] and Kunieda et al. [10], where the matrix cells were linked through additional springs representing the fiber cross. In Schaufert and Cusatis [11], the contribution of the fiber is implemented implicitly in the model.

In this paper, the fiber contribution is implemented through interface elements that represent the fiber-matrix slip.

### 2.1 Mesostructure generation

At the mesolevel, concrete is considered as a random heterogeneous quasi-brittle material with three main phases: mortar, aggregates, and the interfacial transition zone (ITZ).

The mesostructure of concrete is mainly

influenced by the position of coarse aggregates. Therefore, a random distribution of spherical-like particles, simulating the coarse aggregates, is arranged inside the specimen. The particle distribution is made according to a Fuller's curve:

$$P(d) = (d/d_{max})^n \quad (1)$$

where  $P(d)$  is the cumulative percentage passing a sieve aperture diameter  $d$  with respect to the maximum aggregate size  $d_{max}$ ; the exponent in the equation is set to  $n=0.5$ . The total volume of coarse aggregates is assumed to be 40% of the whole concrete volume [13].

Once the particle distribution is generated, following the previous sieve curve, the particles are randomly placed using the take-and-place method [4]. Largest particles are placed first as to preserve locations for smaller particles.

The aggregate arrangement is then used as the input for the Delaunay's triangulation in order to define the matrix mesh [4,7]. It should be remarked this mesh will only depend on the actual material mesostructure.

### 2.2 Fiber generation

The main input for the fiber generation is the volume content which, in addition to the fiber length and diameter, provides the initial number of elements to place in the matrix.

For every single fiber element, an initial node has to be placed randomly within the specimen volume. It is also necessary to define a direction which can be specified or set partially or totally random. This feature is very important to study the effect of fibers direction. If the second node is out of the boundaries, the fiber is automatically cut off at it. The subtracted volume of the fiber is taken into account when placing the next fibers, so as to meet the initial volume content.

Along with the external nodes of the fibers, some internal nodes have to be generated in order to provide the linking to the matrix. These are placed at a certain distance based on the characteristic length of the matrix mesh so as to preserve the characteristic length of the

whole system.

The fiber nodes are linked to the closest aggregates through special interface elements, representing the bond between the concrete matrix and the fibers (Figure 1).

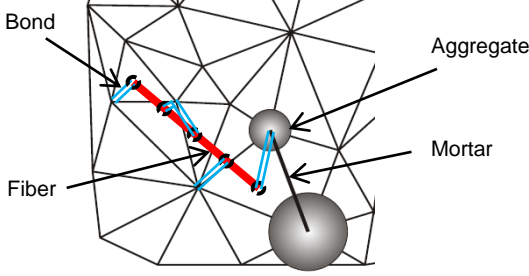


Figure 1: Fiber-reinforced lattice-particle model.

### 2.3 Formulation

In the present formulation of the fiber-reinforced lattice-particle model, three different types of elements can be found: a) matrix; b) fiber; and c) bond; for matrix-matrix, fiber-fiber and fiber-matrix interaction, respectively.

Matrix elements are defined as traditional spring elements acting in normal and tangential directions at a contact point which is proportional to the specific length of the particles [4,5], with the following stiffnesses:

$$\begin{aligned} K_{ij,m}^N &= k_{1,m} E_{ij} A_{ij} / L_{ij} \\ K_{ij,m}^T &= k_{2,m} E_{ij} A_{ij} / L_{ij} \end{aligned} \quad (2)$$

Parameters  $k_{1,m}$  and  $k_{2,m}$  are used to adjust the matrix macroscopic elastic modulus and Poisson's ratio, respectively. Values of  $k_{1,m}=1.0$  and  $k_{2,m}=0.2$  provides a good agreement with experimental data. The length of the element,  $L_{ij}$ , is obtained directly from the Delaunay's triangulation and the area of the element is defined as:

$$A_{ij} = \min(\pi r_i^2, \pi r_j^2) \quad (3)$$

where  $r_i$  and  $r_j$  are the aggregates radii.

Local elastic modulus will depend on the phases of the heterogeneous material: mortar ( $E_m$ ) and aggregates ( $E_a$ ) [7]:

$$\begin{aligned} L_{ij} / E_{ij} &= (r_i + r_j) / E_a + \\ &+ (L_{ij} - r_i + r_j) / E_m \end{aligned} \quad (4)$$

Fiber elements are modeled as simple

trusses with the following normal stiffness:

$$K_{ij,f}^N = E_f A_f / L_f \quad (5)$$

where  $E_f$  is the elastic modulus of the fiber,  $A_f$  the cross-section area ( $A_f = \pi r_f^2$ ) and  $L_f$  the fiber length.

The bond elements are special elements similar to matrix elements which stiffnesses are:

$$K_{ij,b}^N = K_{ij,b}^T = E_b A_b / L_{ij} \quad (6)$$

where  $E_b$  is the elastic modulus of the interface,  $L_{ij}$  the length of the element and  $A_b$  the interaction area defined as follows:

$$A_b = 2\pi r_f L_f \quad (7)$$

Different fracture laws can be found in the literature to account for the fracture behavior of the lattice elements. In this work, a general bilinear material behavior is implemented being necessary to define the peak stresses  $\sigma_1$  and  $\sigma_2$ , and the fracture energy. The shape of the material curve is discussed in the next section.

The material behavior is used within a Mohr-Coulomb failure surface [6] for the matrix and interface elements, and a Rankine criterion for the fibers.

### 2.4 Computational strategy

The system is solved using an event-driven algorithm by which linear steps are solved, making it faster and avoiding major numerical difficulties [9]. At every step, unitary prescribed forces or displacements are applied to the specimen and the element stresses are calculated. The element with the maximum stress-to-strength ratio is supposed to fail and its elastic modulus is updated following the material curve.

The material law is discretized into certain steps; thus, the numerical implementation is straightforward by using a secant reduction approach similar to that of Rots et al. [10].

## 3 PULL-OUT TESTS

The properties of the matrix-fiber interface are difficult to obtain experimentally. For this reason, pull-out tests of the fiber are carried out [2]. In these tests, the fiber is partially

embedded in the matrix and it is pulled-out through the free end (Figure 2).

There are three main stages in a typical force-slip pull-out curve: 1) elastic branch before the chemical bond strength; 2) non-linear fiber-matrix debonding; and 3) frictional softening [2].

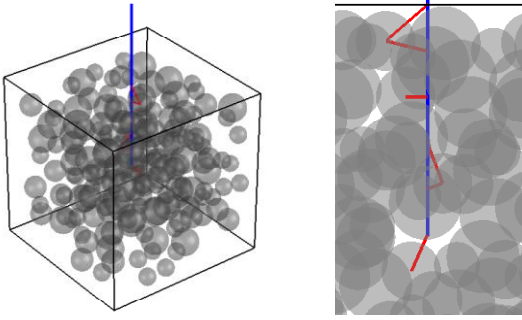


Figure 2: Fiber pull-out configuration.

Different interface behaviors can be found depending on the material type: a) slip hardening; b) elastic-plastic; and c) slip softening. The present model, accounts for all these material behavior through bilinear laws as discussed in section 2.4. The pull-out test configuration used in the simulations is a concrete-matrix cubic specimen of size 50 x 50 x 50 mm, fixed at the bottom surface with a half embedded steel fiber of 50 mm, which is pulled-out by its free end (Figure 3).

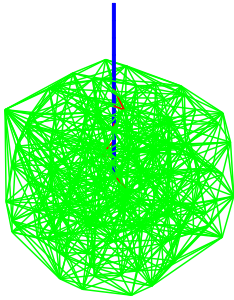


Figure 3: Fiber pull-out test mesh.

The material properties for the interface elements are presented in Table 1. The concrete matrix is modeled as a softening material and the fibers are elastic-plastic (Table 2). In Figure 4 different interface behaviors are compared, showing the ability of the model to account for a wide range of behaviors, from softening to hardening.

Table 1: Interface material properties.

	E (GPa)	$\sigma_1$ (MPa)	$\sigma_2$ (MPa)	$G_D$ (N/mm)
Interface 1	5.0	1.0	0.1	0.035
Interface 2	5.0	1.0	0.9	0.035
Interface 3	5.0	1.0	2.0	0.035

These simulations can be used to calibrate material properties of the fiber-matrix interface in order to study the effect of fiber inclusions on the mechanical properties of the composite material.

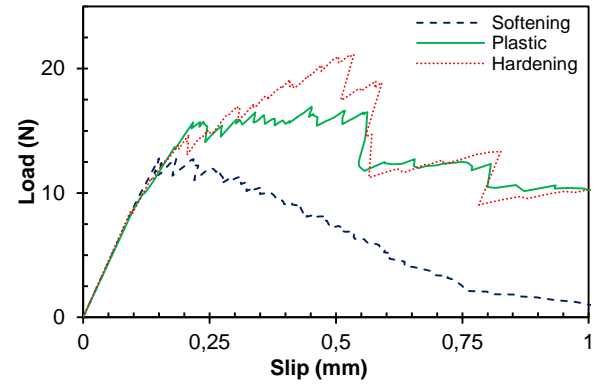


Figure 4: Simulation of the fiber pull-out behavior.

#### 4 TENSILE TESTS

Uniaxial tension tests are suitable for studying the contribution of the fiber reinforcement to the mechanical properties of the new composite material. This change of the ductility is more evident on load-deformation curves and cracking patterns.

For this purpose, a prismatic specimen of size 50 x 25 x 150 mm is subjected to uniaxial tension (Figure 5). The two ends of the specimen are clamped in a width of 25 mm, as usually performed in the laboratory. Normalized stress-strain curves are computed in order to observe the effect of fiber volume content variation and the fiber orientation. The material properties are shown in Table 2.

Different fiber volume content,  $V_f$ , are simulated to show the increase in ductility ( $V_f = 0, 0.5, 1.0$  and  $1.5\%$ ) and the ability to develop distributed cracking (Figure 5). On the other hand, three different types of fiber orientation are accounted for: a) totally random (based on a normal probability

distribution), b) totally aligned along a given direction (loading axis in this case), and c) quasialigned or aligned in a given direction with certain misalignment (maximum  $\pm 10^\circ$ ).

**Table 2:** Material properties.

Matrix	$E_m=20$ GPa, $E_a=70$ GPa $f_t=4$ MPa, $f_c=-80$ MPa $c=2f_t$ , $\phi=35^\circ$ , $G_F=0.02$ N/mm
Fiber	$E_f=210$ GPa $\sigma_{y1}=510$ MPa, elastic-plastic $L_f=50$ mm, $d_f=0.5$ mm Variable $V_f$ and alignment
Interface	$E_b=5$ GPa $\sigma_{I1}=1.0$ MPa, $\sigma_{I2}=0.1$ MPa $c=2\sigma$ , $\phi=35^\circ$ , $G_D=0.035$ N/mm

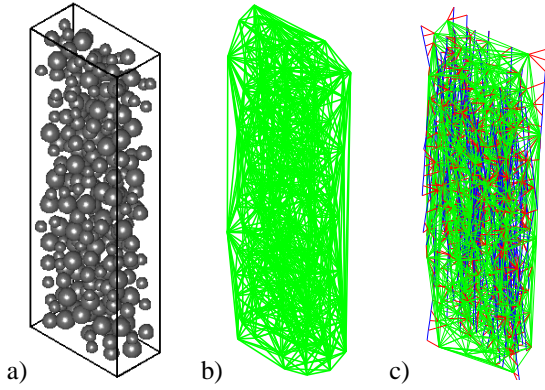


**Figure 5:** Uniaxial tension test : a) particles distribution, b) matrix mesh, and c) fiber mesh.

As mentioned before, the present model is able to account for distribute cracking when present. In Figure 6 the displacement fields for two volume contents are compared at a total longitudinal strain of 0.15%. It can be seen that, in the case of low fiber content ( $V_f=0.5\%$ ), a single crack is developed and presented as a displacement jump. However, if the fiber content is increased ( $V_f=1.5\%$ ), the displacement field is still distributed. The cracks are generally presented as vertical stress drops in stress-strain curves.

The increase in ductility is achieved by the arresting effect that fibers have in the matrix. Therefore, fibers are expected to arrest the cracks, increasing the strain capacity of the material (Figure 7).

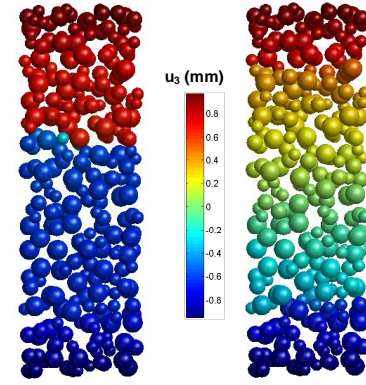


**Figure 6:** Displacement field at 0.15 % global strain: a)  $V_f=0.5\%$ , and b)  $V_f=1.5\%$ .

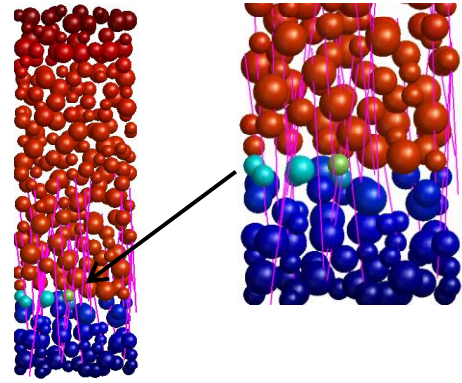


**Figure 7:** Acting fibers arresting a crack.

#### 4.1 Effect of $V_f$

The increase of the fiber volume content should increase the ductility in the composite material. This observation is analyzed with the proposed model and by comparing four different contents: a) plain concrete ( $V_f=0\%$ ), b)  $V_f=0.5\%$ , c)  $V_f=1.0\%$ , and d)  $V_f=1.5\%$ . The fibers are quasialigned distributed with a maximum misalignment of  $10^\circ$ .

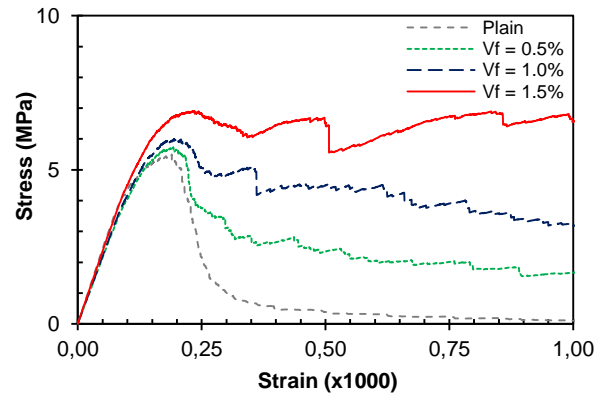


**Figure 8:** Effect of the fiber volume content.

In Figure 8 it is observed that the model

predicts well the experimental observations. The increase of the fiber content gradually increases the peak stress and the fracture energy of the material. The softening shape is lost, showing a ductile-like behavior in the case of high fiber volume content. It can be also observed that the strain capacity increases in the same manner.

#### 4.2 Effect of fiber orientation

One important aspect to analyze when dealing with fiber-reinforced composites is the effect of the fiber orientation. In fact, this is a key issue in order to achieve better performances of the material. Different fiber distributions are considered in this paper (Figure 9).

The best behavior of the composite is expected to happen when the fibers are perpendicular to the crack path (Figure 9c), so the fiber contribution to the arresting is the most. However, this perfectly aligned configuration is hard to obtain in situ due to certain misalignment given by the casting flow. Therefore, fibers with a maximum misalignment of  $10^\circ$  along the loading axis are simulated in order to account for such effect (Figure 9b). Another configuration considered in this work is to have a completely random fibers distribution (Figure 9a).

For these simulations, the material properties in Table 2 are used and a total fiber volume content of 0.5% is considered. Uniaxial tension tests are carried out and normalized stress-strain curves, as in the previous section, were obtained.

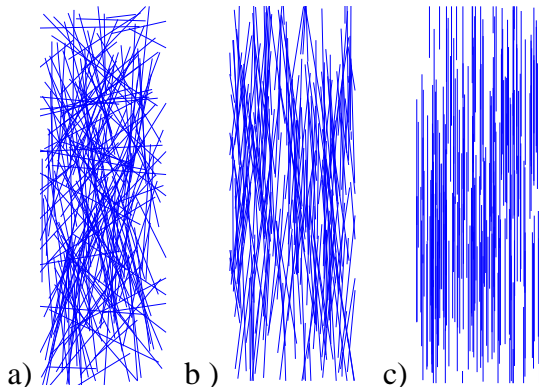


Figure 9: Fiber distributions: a) random, b) quasialigned, and c) aligned.

From the uniaxial curves in Figure 10, it is observed that the fiber orientation has its effects on material response. Indeed, an increase on the alignment level leads to low increase of the peak-stress and an important increase of the ductility. In Figure 10 this effect is observed, being the random configuration under the quasialigned and aligned specimens. The difference between the quasialigned and the perfectly aligned configuration is not much. Therefore, for concrete, it would not be necessary to have a perfect alignment, since a misalignment of  $10^\circ$  seems to provide good results close to the ideal case. The strain capacity is also higher for the quasialigned and perfectly aligned cases, obtaining almost twice the bearing capacity at a strain level of 0.1%.

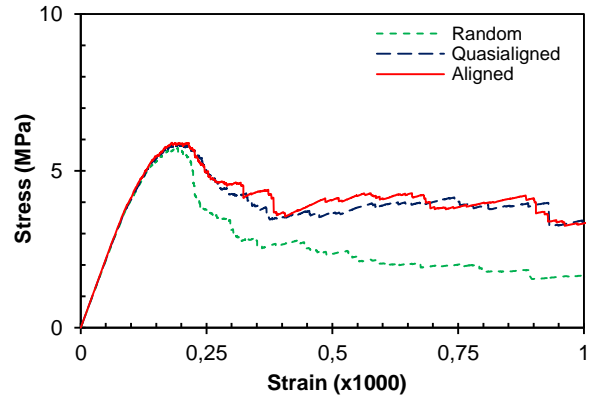


Figure 10: Effect of the fiber alignment.

## 5 CONCLUSIONS

The use of FRHPC is nowadays widely extended, and there exists a need to develop numerical tools to aid the material engineers in the design and structural prediction of these types of materials.

In this paper, a three-dimensional fiber-reinforced lattice-particle model is presented to simulate the mechanical behavior of FRHPC. The proposed model is based on the interaction of aggregates and fiber through interface elements that are especially characterized with pull-out tests. Different fiber distributions are generated according to a given set of geometrical parameters (e.g. fiber length and diameter, volume content, orientation). This information along with the

results from the pull-out tests are implemented into direct tension tests to analyze the material behavior under different fiber configurations.

From the results in Section 4, we can conclude the model is able to reproduce fracture processes in fiber-reinforced cementitious composites. Moreover, it has shown agreement with the experimental observations regarding the effect of the fiber volume content and fiber orientation. Different types of material behaviors can be represented, ranging from softening to hardening, modifying the ductility and the peak-stress. This depends on the aforementioned configurations.

In general, the increase of the fiber volume fraction leads to an increase of the ductility of the material. This increase can also transform the material behavior from a quasi-brittle to a ductile material. For the type of fibers tested in this work, volume contents over 1% seem to be enough as to strongly improve the mechanical response. On the other hand, from the fiber orientation results, it is remarkable that the improvement obtained by perfectly aligning the fibers is not too high with respect to a quasialigned configuration. Taking in consideration the cost increments of a perfectly aligned configuration, it makes not worthy to have such distribution, at least for concrete.

This model opens new future research work in many directions. The implementation of other type of setups as well as different type of fibers is of main interest. One important objective is the calibration of the model with experimental results in order to validate it.

## REFERENCES

- [1] Li, V.C. 2003., On engineered cementitious composites (ECC) – A review of the material and its applications. *J. Adv. Con. Tech.*, **1(3)**:215-230.
- [2] Bentur, A. and Mindess, S., 2007. *Fibre Reinforced Cementitious Composites*. Taylor&Francis.
- [3] Schlangen, E. and van Mier, J.G.M., 1992. Experimental and numerical analysis of micromechanisms of fracture cement-based composites. *Cem. Con. Comp.*, **14**:105-118.
- [4] Bažant, Z.P., Tabbara, M.R., Kazemi, M.T. and Pijaudier-Cabot, G., 1990. Random particle model for fracture of aggregate of fiber composites. *ASCE J. Eng. Mech.*, **116(8)**:1686-1705.
- [5] Zubelewicz, A. and Bažant, Z.P., 1987. Interface element modeling of fracture in aggregate composites. *J. Eng. Mech.*, **113(11)**:1619-1630.
- [6] Bolander, J.E. and Saito, S., 1998. Fracture analysis using spring network with random geometry. *Engrg. Frac. Mech.*, **61(5-6)**:569-591.
- [7] Cusatis, G., Bažant, Z.P. and Cedolin, L., 2003. Confinement-shear lattice model for concrete damage in tension and compression: I. Theory. *J. Eng. Mech.*, **129(12)**:1439-1448.
- [8] Schlangen, E., Qian, Z., Sierra-Beltrán, M.G. and Zhou, J., 2009. Simulation of fracture in fibre cement based materials with a micro-mechanical lattice model. *Proc. 12<sup>th</sup> International Conference on Fracture*, Canada, 2009.
- [9] Bolander, J.E. and Saito, S., 1997. Discrete modeling of short-fibers reinforcement in cementitious composites. *Advn. Cem. Bas. Mat.*, **6**:76-86.
- [10] Kunieda, M., Ogura, H., Ueda, N. and Nakamura, H., 2011. Tensile fracture process of strain hardening cementitious composites by means of three-dimensional meso-scale analysis. *Cem. Con. Comp*, **33**:956-965.
- [11] Schauffert, E. and Cusatis, G., 2012. Lattice discrete particle model for fiber-reinforced concrete: I. Theory. *J. Eng.*

*Mech.*, **138(7)**:826-833.

- [12] Montero, F. and Schlangen, E., 2012. Modelling of fracture in fibre-cement based materials. Tenth International Symposium on Brittle Matrix Composites, Oct. 15-17, 2012, Warsaw, Poland.
- [13] Wriggers, P. and Moftah, S.O., 2006. Mesoscale models for concrete: Homogenisation and damage behavior. *Finite Elem. Anal. Des.*, **42**:623-636.
- [14] Schlangen, E. and Garboczi, E.J., 1997. Fracture simulations of concrete using lattice models: computational aspects. *Eng. Frac. Mech.*, **57(2)**:319-332.
- [15] Rots, J.G. and Invernizzi, S., 2004. Regularized sequentially linear saw-tooth softening model. *Int. J. Numer. Anal. Meth. Geomech.*, **28**:821-856.